Electronic Ferroelectricity in a Molecular Crystal with Large Polarization Directing Antiparallel to Ionic Displacement

Kensuke Kobayashi,[1,*] Sachio Horiuchi,[2,3,†] Reiji Kumai,[1,2] Fumitaka Kagawa,[3,4] Youichi Murakami,[1] and Yoshinori Tokura[2,4,5]

[1]*Condensed Matter Research Center (CMRC) and Photon Factory, Institute of Materials Structure Science, High Energy Accelerator Research Organization (KEK), Tsukuba, 305-0801, Japan*
[2]*National Institute of Advanced Industrial Science and Technology (AIST), Tsukuba, 305-8562, Japan*
[3]*CREST, Japan Science and Technology Agency (JST), Tokyo 102-0076, Japan*
[4]*Department of Applied Physics, University of Tokyo, Tokyo 113-8656, Japan*
[5]*Correlated Electron Research Group (CERG) and Cross-Correlated Materials Research Group (CMRG), ASI-RIKEN, Wako 351-0198, Japan*

(Received 6 March 2012; published 4 June 2012)

Ferroelectric polarization of 6.3 μC cm^{-2} is induced by the neutral-to-ionic transition, upon which nonpolar molecules of electron donor tetrathiafulvalene (TTF) and acceptor *p*-chloranil (CA) are incompletely ionized to $\pm 0.60e$ and dimerized along the molecular stacking chain. We find that the ferroelectric properties are governed by intermolecular charge transfer rather than simple displacement of static point charge on molecules. The observed polarization and poling effect on the absolute structural configuration can be interpreted in terms of electronic ferroelectricity, which not only exhibits antiparallel polarity to the ionic displacement but also enhances the polarization more than 20 times that of the point-charge model.

DOI: 10.1103/PhysRevLett.108.237601 PACS numbers: 77.80.-e, 61.05.cp, 71.20.Rv, 77.84.Jd

Switchable large polarization of ferroelectrics has opened the way to electronics applications such as a capacitor, sensor, and data storage, as well as to electromechanical and optical devices [1–3]. Whereas the sum of permanent dipole moments of polar ions determines the polarization of orientational ''order-disorder-type'' ferroelectrics, the product of relative displacement and charge of the ions had been the classical picture of the polarization for the ''displacive-type'' ferroelectrics. In actual ferroelectrics, however, even accurate knowledge of spatial charge distributions, which can be obtained in principle by the precise x-ray structural analysis, cannot explain the macroscopic polarization quantitatively. The electric polarization can be correctly represented on the basis of the quantum mechanical theory using the formalism of Berry phase by calculating the displacement current under changes of the electronic wave functions [4,5]. This fact is especially important for the displacive-type ferroelectrics having some orbital hybridization between ions [6,7]. In this context, recent first-principles calculations with full consideration of Berry phase have greatly advanced understanding of the dielectrics. For instance, the displacive-type ferroelectric oxides have disclosed the importance of electronic effect, which amplifies the macroscopic polarization through the orbital hybridization between the occupied *p*-orbitals of oxygen and the empty *d*-orbitals of transition metals [8].

Here we address the extreme case that the electronic process mostly governs the large polarization of a ferroelectric. The compound focused herein is an organic charge-transfer complex of electron donor (D), tetrathiafulvalene (TTF) and acceptor (A), *p*-chloranil (CA) [Fig. 1] [9]. The primary characteristic of this compound is a valence instability called the neutral-to-ionic transition

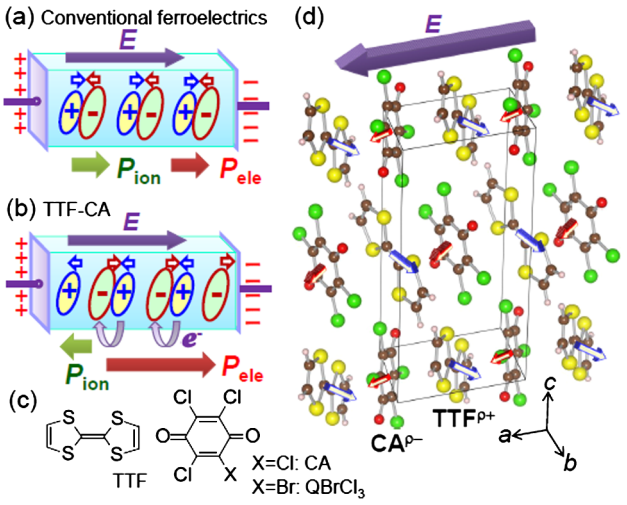

FIG. 1 (color online). Schematic illustrations of the electric polarization (solid arrows) and displacement direction (small open arrows) of ions in the conventional displacive-type ferroelectrics (a) and the TTF-CA crystal (b). The positively charged TTF and negatively charged CA acceptor molecules are displaced against the electric field. Bent arrows denote the electric charge-transfer process from TTF to CA. (c) Molecular structures of TTF, CA, and $QBrCl_3$. (d) Crystal structure of TTF-CA and molecular displacement directions under electric field.

(NIT), which arises from a delicate balance between the electrostatic energy gain and the energy cost of molecular ionization [9,10]. According to the C = O stretch mode vibration frequency in the infrared spectra, averaged molecular ionicity ρ was found to jump from ~0.3 for the quasineutral phase to ~0.6 for the quasi-ionic phase upon the NIT [Fig. 2(a)] [11,12].

The TTF-CA crystal comprises the *DA* alternating stacks along the *a* axis [13] and the one-dimensional nature along this chain brings about the structural instability of Peierls or spin-Peierls type, displacing pairwise the ionized *D* and *A* molecules [Fig. 1(d)]. Ferroelectricity emerges if the chain can invert its polarity as $..\underline{DA}\,\underline{DA}.. \leftrightarrow ..\underline{AD}\,\underline{AD}...$, where the underlines represent the dimerized *DA* pairs [14] The crystal structure is symmetry-broken to a polar space group of *Pn* upon NIT as determined by the neutron [15] and high-resolution x-ray diffraction [16] experiments. The recent microscopic electroreflectance spectroscopy revealed coexisting domains of different polarities [17], whereas pyroelectric measurement proved the existence of spontaneous polarization for the monobromine-substituted isomorph, TTF-$QBrCl_3$ (2-bromo-3,5,6-trichloro-*p*-benzoquinone) [18].

The TTF-CA complex can be regarded as a displacive-type ferroelectric because the molecules remain flat and nearly symmetric in form; the dipole moments of both TTF and CA are negligibly small (< 0.1 Debye) according to the semiempirical molecular orbital calculations with the parametric method 3 (PM3) Hamiltonian and restricted Hatree-Fock (RHF) method using the MOPAC program [19]. The molecular charge $Ze = \pm 0.60(3)e$ and relative displacement $\mathbf{u} = [+0.110(1), -0.023(1), +0.035(2)]$ Å along the crystallographic ($\boldsymbol{a}$, $\boldsymbol{b}$, $\boldsymbol{c}$) direction [16] yield a dipole moment of $\boldsymbol{\mu}^{(\mathrm{cell})} = \Sigma_{(\mathrm{cell})} Ze\mathbf{u} = [0.62(3), 0, 0.20(3)]$ Debye per one unit cell (volume $V_{\mathrm{cell}} = 779.02(13)$ Å^3), which corresponds to the small ionic polarization of $\mathbf{P}^{\mathrm{ion}} = \boldsymbol{\mu}^{(\mathrm{cell})}/V_{\mathrm{cell}} = [0.27(2), 0, 0.09(2)]$ μC cm^{-2} at $T = 15$ K [20]. In contrast to this conventional point-charge picture, the recent first-principles calculations invoked a much larger spontaneous polarization (3–10 μC cm^{-2} along the *a* direction) with two contrasting candidates of electronic states [21,22]; the total polarization is predicted to direct either parallel or antiparallel to the ion polarization, depending on the antiferromagnetic or nonmagnetic state, namely, the presence or absence of the $S = 1/2$ spins on each ionized molecule. (Note however that there is no antiferromagnetic state realized even in the "ionic" *DA* stacks because of the spin singlet formation on the *DA* dimerized lattice.) Such predictions strongly motivated us to experimentally determine both the magnitude and the direction of spontaneous polarization.

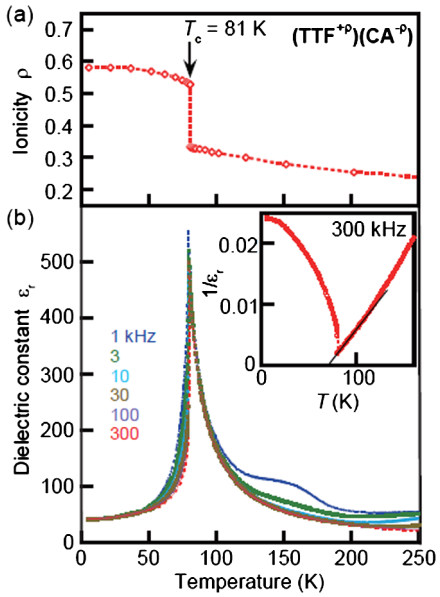

FIG. 2 (color online). Temperature-dependent properties of TTF-CA. (a) Change of ionicity probed by the C = O stretch mode frequency of the CA molecule. (b) Relative permittivity measured along the crystal *a* direction. The inset shows the temperature dependence of inverse permittivity ($f = 300$ kHz) with a fit (straight line) to the Curie-Weiss law.

The ferroelectric nature of NIT becomes evident by a sharp peak anomaly on the temperature-dependent permittivity. In the currently reexamined permittivity data [Fig. 2(b)], the dielectric relaxation seen at temperatures around 130–170 K is much lower than the previous report [23]. This contribution, which arises from the low-frequency bound motion of locally pinned polar domains, was minimized on the freshly prepared crystals with the least mechanical stress. Thereby, the curvature showed the well-defined Curie-Weiss behavior, $\varepsilon_r = C/(T - \theta)$, prior to the NIT. The linear $1/\varepsilon_r$-T relationship at high frequency (300 kHz) [Fig. 2(b)] deduces the Curie constant C (5.0×10^3 K) and Weiss temperature θ (69.9 K), and the large discrepancy between T_c and θ is indicative of the strong first-order nature of NIT.

The large ε_r and C are suggestive of a large spontaneous polarization as a proper ferroelectric. Nevertheless, its narrow charge gap of TTF-CA (~ 0.7 eV) gives rise to an incompletely insulating electric resistivity as low as $\sim 10^{-8}$ Ω cm^{-1} [24], even at low temperatures around T_c, and has long hindered the experimental evaluation of the spontaneous polarization value. Additional electric leakage under the higher field comes from the nonlinear electric transport and the current-induced resistance switching to a low-resistance state when the external electric field exceeds approximately 10 kV cm^{-1} [25]. For this reason, the maximum field was limited to this value in the polarization hysteresis measurement, and its satisfactory observations required further cooling. This is contrasted by the case of TTF-$QBrCl_3$, which shows better insulating properties (~ 10^{10} Ω cm), enabling the clear observation of *P*-*E* hysteresis even at around T_c (~ 71 K) [Fig. 3(a)]. As exemplified by the 51 K data in Fig. 3(b), the rectangular *P*-*E*

curvature at high frequencies well proves the ferroelectricity, although it turns to the longitudinally warped one due to the electric leakage with decreasing frequency to 10 Hz. On the other hand, the coercive field E_c increases with increasing frequency or lowering temperature probably due to the rate-limiting domain-wall dynamics. Satisfactory observations of hysteresis were thereby limited in a narrow range of both frequency and temperature.

The large spontaneous polarization was further validated by eliminating the nonhysteresis contributions in the *P-E* hysteresis using a double triangular waveform voltage for the positive-up-negative-down (PUND) procedure [Fig. 3(c) and 3(d)]. Whereas the positive and negative inputs reverse the polarization, the up and down inputs retaining the polarity can extract nonhysteresis contributions such as electric leakage and the linear dielectric (capacitance) component by a nonlinear current-voltage relationship for electric leakage. Elimination of these effects showed a well-defined parallelogramlike hysteresis [solid curve in Fig. 3(c)] of the P_r of 6.3 μC cm^{-2} and E_c of 5.4 kV cm^{-1} at $T = 59$ K. The ferroelectricity of TTF-$QBrCl_3$ was confirmed similarly by this procedure ($P_r = 6.7$ μC cm^{-2}, $E_c = 4.5$ kV cm^{-1} at $T = 56$ K). This also ensures that the TTF-CA derivatives show generic and proper ferroelectric transitions upon their NITs. The flat curvature in the bottom and top of the loop indicates a good agreement between the remanent and saturated polarizations, namely, the negligible polarization decay in one period of the measurements (< 0.1 sec).

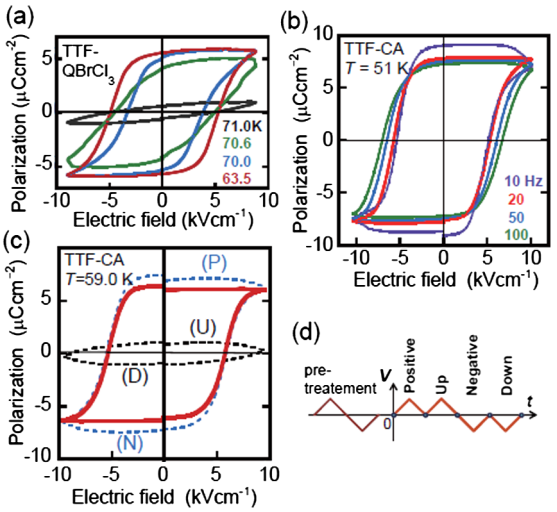

FIG. 3 (color online). The polarization measured with triangular ac electric field ($E \| a$). (a) *P-E* hysteresis loops of TTF-$QBrCl_3$ at various temperatures. (b) Hysteresis loops of TTF-CA with various frequencies at 51 K. (c) The *P-E* curves of TTF-CA using the positive-up-negative-down procedure with a double triangular waveform voltage ($f = 500$ Hz, $T = 59$ K) [illustrated on (d)]. The purely hysteresis component (solid curve) was obtained by subtracting the nonhysteresis contributions (up and down runs) from the total ones (positive and negative runs).

The ionic polarization involves a finite *c*-direction component by symmetry, as noted above ($P_x^{\text{ion}} \approx 3P_z^{\text{ion}}$). In contrast, the total polarization P_s observed has a negligibly small *c*-direction component, as indicated by a nearly temperature-independent permittivity and a silent *P-E* hysteresis, and then the direction P_s is regarded as parallel to the *DA*-stacking *a* axis. Conversely, the observation of such highly unidirectional P_s indicates that the conventional ionic displacement plays a minor role in the emergence of ferroelectricity in the present compounds.

Here we argue the relation between the observed spontaneous polarization and Curie constant for TTF-CA. The unit cell contains two *DA* pairs and the density of dipoles ($N = 2/V_{\text{cell}}$) is 2.461×10^{27} m^{-3}. The effective paraelectric moment μ_C ($\approx 1.6 \times 10^{-29}$ C m) per formula unit as derived from $C = N\mu_C^2/k_B\varepsilon_0 = 5.0 \times 10^3$ K (k_B, Boltzmann constant; ε_0, permittivity of vacuum) is comparable to the moment $\mu_s = P_r/N$ ($\approx 2.6 \times 10^{-29}$ Cm) calculated from the remanent polarization P_r (≈ 6.3 μC cm^{-2}). For the TTF-$QBrCl_3$ crystal of $N = 2.414 \times 10^{27}$ m^{-3}, $P_r = 6.7$ μC cm^{-2}, and $C = 6.4 \times 10^3$ K, we obtained the similar moments $\mu_C \approx 1.8 \times 10^{-29}$ Cm and $\mu_s = 2.8 \times 10^{-29}$ Cm. Whereas μ_C and μ_s almost coincide with each other for the order-disorder-type ferroelectricity of permanent dipoles, the displacive-type ferroelectrics exhibit the different relation, $r = \mu_C/\mu_s \sim 2$ [26]. Here we found an unexpected relation, $r = 0.62 < 1$ for TTF-CA (0.65 for TTF-$QBrCl_3$) [27,28]. This might reflect the distinct electronic origins between the neutral paraelectric state for μ_C and the ionic ferroelectric state for μ_s.

The symmetry-breaking of TTF-CA crystal structure under the electric field was probed by the intensity difference between Bijvoet pair (hkl vs $\bar{h}\bar{k}\bar{l}$) reflections, which arises from the anomalous x-ray scattering effect [20,29]. The simulation based on the crystal structures at $T = 15$ and 40 K [15,16] predicts that the Bijvoet pair reflections 101 and $\bar{1}0\bar{1}$ have sufficient intensities and are the most susceptible to the anomalous x-ray scattering for x-ray wavelength $\lambda = 1.55$ Å used. Figure 4(a) depicts the temperature dependence of their normalized integrated intensity $I_+ \equiv I(101)/\{I(101) + I(\bar{1}0\bar{1})\}$ and $I_- \equiv I(\bar{1}0\bar{1})/\{I(101) + I(\bar{1}0\bar{1})\}$. The crystal was cooled under the poling electric field of $+4$ kV cm^{-1} applied along the crystal *a* direction. Note that the applied field is defined as plus when directing to the crystal *a* direction. For temperatures above $T_c = 81$ K, this reflection intensity obeys Friedel's law, $I_+ = I_- = 0.5$, expected for the centric (paraelectric) structure free from the anomalous x-ray scattering. Below T_c, one of the I_+ and I_- decreases from 0.5 and the other increases, indicating the symmetry breaking with the strong first-order nature. The I_+ and I_- of the Bijvoet pair were interchanged by inverting the electric field direction due to polarization switching, as exhibited for $T = 61$ K in Fig. 4(b).

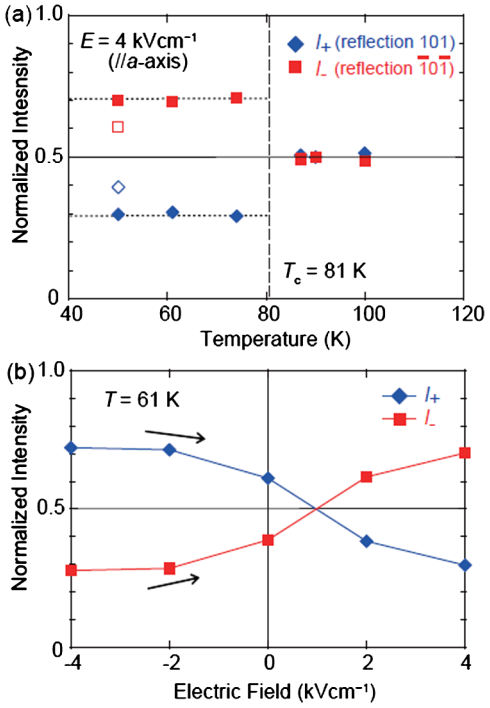

FIG. 4 (color online). Degree of bulk polarization under electric field $E(\|a)$ probed by the anomalous x-ray scattering effect. (a) Temperature dependence of normalized integrated intensity $I_+ \equiv I(101)/\{I(101) + I(\bar{1}0\bar{1})\}$ and $I_- \equiv I(\bar{1}0\bar{1})/\{I(101) + I(\bar{1}0\bar{1})\}$ of Bijvoet pair reflections 101 and $\bar{1}0\bar{1}$ at constant $E = +4\ \mathrm{kV\,cm^{-1}}$. Open symbols are intensity data measured at 32 min after switching off to $E = 0$ at $T = 50$ K and represent a polarization decay toward the multidomain state. (b) Normalized intensity I_+ and I_- under E increasing from $-4\ \mathrm{kV\,cm^{-1}}$ to $+4\ \mathrm{kV\,cm^{-1}}$ at 61 K. Switching of the polarization interchanges their magnitudes with each other at $E \sim 1\ \mathrm{kV\,cm^{-1}}$.

Just below T_c, the observed I_+ and I_- approach 0.705 or 0.295 [horizontal dotted lines in Fig. 4(a)], which corresponds to the full polarization into either polarity according to the simulation. Therefore, the poling field of $4\ \mathrm{kV\,cm^{-1}}$ is sufficient for developing a single-domain state. The intensity difference developed below T_c is almost independent of temperature variation, in agreement with the fact that magnitude of polarization of $6.7\ \mu\mathrm{C\,cm^{-2}}$ depends little on temperature as directly observed for TTF-$QBrCl_3$ [Fig. 3(a)].

Here we note the polarization decay, which was invisible in the dynamical measurement of the P-E loop [Fig. 3]. As exhibited in Fig. 4(b), the difference between I_+ and I_- gradually decreases with decreasing field E and $I_+ = I_- = 0.5$ for equal volume fractions of domains appears at $E \sim 1\ \mathrm{kV\,cm^{-1}}$, which is much smaller than coercive field $E_c \sim 4\ \mathrm{kV\,cm^{-1}}$. These discrepancies may originate from the different time scale of measurements; the x-ray diffraction was a quasistatic measurement, taking about 32 min for each diffraction image, whereas the hysteresis experiment completed within 0.1 sec. Then, the polarization decay process is as slow as a second to a minute, although more precise understanding requires further studies in detail. The degree of depolarization somewhat depends on crystals; for the crystal shown in Fig. 4(a), the portion of about 25% spontaneously reversed its polarity after the applied electric field was removed.

By comparing the observed intensity of Bijvoet pair (I_+ and I_-) with the simulation, we identified the absolute configuration of the crystal structure relative to the externally applied field. The positively charged TTF molecules shift toward the positive electrode and the negatively charged CA toward the negative electrode. The configuration with all the ionic charges displacing against the electric field is counterintuitive for the displacive-type ferroelectrics. Considering that the strong electric field always compels the aligning of the total spontaneous polarization P_s in the same direction, P_s should direct antiparallel to the ionic displacement. This picture is in accord with the theoretical prediction assuming the nonmagnetic state rather than antiferromagnetic one [21,22].

At the earliest stage of research, the NIT was described by an electrostatic picture of Madelung energy gain vs ionization energy of molecules [9,10]. In contrast, the classical point-charge picture completely fails to explain both the magnitude and polarity of polarization. Here we consider the origin of this large discrepancy. Judging from negligible molecular dipole moments and tiny ionic polarizations herein, a major contribution to the spontaneous polarization should be the electronic polarization. In the displacive-type ferroelectric oxides, Born effective charge Z^*, which relates the change of polarization $\mathbf{\Delta P}$ with displacement $\mathbf{u}$ as $\mathbf{\Delta P} = Z^* e\mathbf{u}/V_{\mathrm{cell}}$, is enhanced by strong orbital hybridization, as compared to the formal valence state of ions. For instance in $PbTiO_3$, the first-principles calculations revealed $Z^*(\mathrm{Ti}^{4+}) = +7.06$ and $Z^*(\mathrm{O}^{2-}) = -5.83$ or -2.56 for $\mathbf{u}\|\langle 100\rangle$ [8]. The TTF-CA system appears to be the extreme case exhibiting the colossal Z^* of opposite sign in comparison with the respective molecular valence (± 0.60); $Z^*(D) = -13.9$ and $Z^*(A) = +13.9$ were roughly estimated from relative displacement $u_x = 0.110$ Å and observed polarization $P_x = 6.3\ \mu\mathrm{C\,cm^{-2}}$ through $P_x = 2Z^* e u_x/V_{\mathrm{cell}}$. Actually, the highest occupied molecular orbital (HOMO) of TTF strongly hybridized with the lowest unoccupied one (LUMO) of CA, as evidenced by the large electron transfer interaction t (~ 0.24 eV) deduced by optical spectra [30].

Closely related issues were also argued by Soos *et al.* [31,32], who have analyzed $\partial P/\partial\delta$, the partial derivative of electric polarization with the dimerization (displacement) amplitude δ within a modified Peierls-Hubbard model. They found that the sign of charge flux $\partial P/\partial\delta$ changes from negative to positive with increasing ρ from the neutral (nonmagnetic) to ionic (magnetic) side. This finding is compatible with the first-principles calculations

[21] predicting the directional change of total polarizations between the antiferromagnetic and nonmagnetic electronic states. For this reason, Soos *et al.* pointed out that the transfer integral, namely, the covalency, increases and changes the degree of charge transfer with dimerization [32]. With these pictures applied to our case, the *DA* dimerization upon the NIT increases the ionicity ρ through the electron transfer along the stack as illustrated by bent arrows in Fig. 1(b), producing the very large polarization.

In conclusion, the colossal effective Born charges of opposite signs of the constituent ions strongly indicate the genuine "electronic ferroelectricity" in the nominally ionic molecular compound TTF-CA. Such an electronic process governs the magnitude and even the direction of macroscopic polarization. The electronic ferroelectricity itself is one of the emerging phenomena in the correlated electron system, such as the charge-ordered ferroelectrics and spin-driven ferroelectrics called multiferroics [33]. The electronic response with less energetic cost of lattice deformations in the present molecular system will promise both high-performance and high-frequency operations as well as new functionalities, e.g., related to nonlinear- or electro-optics [17]. For high-functional ferroelectricity in a molecular system, we remark that substantial covalency between interacting molecular orbitals can be the key to overcoming the small ionic charge, dilute dipole density inherent to molecular crystals, and even the least permanent molecular dipoles.

We thank S. Ishibashi and H. Okamoto for enlightening discussions. The synchrotron x-ray study was performed with approval of the Photon Factory Program Advisory Committee (No. 2009S2-003). This work was partially supported by the Japan Society for the Promotion of Science (JSPS) through Funding Program for World-Leading Innovative R&D on Science and Technology (FIRST Program), by KAKENHI (No. 20110003 from MEXT and No. 23340111 from JSPS), and by grants-in-aid from the Sumitomo Foundation.

*kensuke.kobayashi@kek.jp
†s-horiuchi@aist.go.jp

[1] K. Uchino, *Ferroelectric Devices* (Marcel Dekker, New York 2000).
[2] M. E. Lines and A. M. Glass, *Principles and Applications of Ferroelectrics and Related Materials* (Oxford University, New York 1977).
[3] J. F. Scott, Science **315**, 954 (2007).
[4] R. D. King-Smith and D. Vanderbilt, Phys. Rev. B **47**, 1651 (1993).
[5] R. Resta, Rev. Mod. Phys. **66**, 899 (1994).
[6] R. E. Cohen, Nature (London) **358**, 136 (1992).
[7] T. Egami, S. Ishihara, and M. Tachiki, Science **261**, 1307 (1993).
[8] W. Zhong, R. D. King-Smith, and D. Vanderbilt, Phys. Rev. Lett. **72**, 3618 (1994).
[9] J. B. Torrance, J. E. Vazquez, J. J. Mayerle, and V. Y. Lee, Phys. Rev. Lett. **46**, 253 (1981).
[10] H. M. McConnell, B. M. Hoffman, and R. M. Metzger, Proc. Natl. Acad. Sci. U.S.A. **53**, 46 (1965).
[11] A. Girlando, F. Marzola, C. Pecile, and J. B. Torrance, J. Chem. Phys. **79**, 1075 (1983).
[12] S. Horiuchi, Y. Okimoto, R. Kumai, and Y. Tokura, J. Phys. Soc. Jpn. **69**, 1302 (2000).
[13] J. J. Mayerle, J. B. Torrance, and J. I. Crowley, Acta Crystallogr. Sect. B **35**, 2988 (1979).
[14] Y. Tokura, S. Koshihara, Y. Iwasa, H. Okamoto, T. Komatsu, T. Koda, N. Iwasawa, and G. Saito, Phys. Rev. Lett. **63**, 2405 (1989).
[15] M. Le Cointe, M. H. Lemee-Cailleau, H. Cailleau, B. Toudic, L. Toupet, G. Heger, F. Moussa, P. Schweiss, K. H. Kraft, and N. Karl, Phys. Rev. B **51**, 3374 (1995).
[16] P. García, S. Dahaoui, C. Katan, M. Souhassou, and C. Lecomte, Faraday Discuss. **135**, 217 (2007).
[17] H. Kishida, H. Takamatsu, K. Fujinuma, and H. Okamoto, Phys. Rev. B **80**, 205201 (2009).
[18] F. Kagawa, S. Horiuchi, H. Matsui, R. Kumai, Y. Onose, T. Hasegawa, and Y. Tokura, Phys. Rev. Lett. **104**, 227602 (2010).
[19] J. J. P. Stewart, Int. J. Quantum Chem. **58**, 133 (1996).
[20] See Supplemental Material at http://link.aps.org/supplemental/10.1103/PhysRevLett.108.237601 for detailed x-ray diffraction experiments and the point-charge-model calculations.
[21] G. Giovannetti, S. Kumar, A. Stroppa, J. van den Brink, and S. Picozzi, Phys. Rev. Lett. **103**, 266401 (2009).
[22] S. Ishibashi and K. Terakura, Physica B (Amsterdam) **405**, S338 (2010).
[23] H. Okamoto, T. Mitani, Y. Tokura, S. Koshihara, T. Komatsu, Y. Iwasa, T. Koda, and G. Saito, Phys. Rev. B **43**, 8224 (1991).
[24] T. Mitani, Y. Kaneko, S. Tanuma, Y. Tokura, T. Koda, and G. Saito, Phys. Rev. B **35**, 427 (1987).
[25] Y. Tokura, H. Okamoto, T. Koda, T. Mitani, and G. Saito, Phys. Rev. B **38**, 2215 (1988).
[26] M. Tokunaga, J. Phys. Soc. Jpn. **57**, 4275 (1988).
[27] It should be noted that the observed electric susceptibility in the paraelectric state (i.e. μ_C) is already enhanced by the correlation effect of about 10*DA* pairs extending along the stack as observed in an x-ray diffuse scattering experiment [28].
[28] M. Buron-Le Cointe, M. H. Lemée-Cailleau, H. Cailleau, S. Ravy, J. F. Bérar, S. Rouzière, E. Elkaïm, and E. Collet, Phys. Rev. Lett. **96**, 205503 (2006).
[29] J. M. Bijvoet, A. F. Peerdeman, and A. J. Bommel, Nature (London) **168**, 271 (1951).
[30] A. Painelli and A. Girlando, J. Chem. Phys. **87**, 1705 (1987).
[31] L. Del Freo, A. Painelli, and Z. G. Soos, Phys. Rev. Lett. **89**, 027402 (2002).
[32] Z. G. Soos, S. A. Bewick, A. Peri, and A. Painelli, J. Chem. Phys. **120**, 6712 (2004).
[33] S. Ishihara, J. Phys. Soc. Jpn. **79**, 011010 (2010).